# dcemri: A Package for Medical Image Analysis

Brandon Whitcher
bjw34032@users.sourceforge.net
Volker J. Schmid
volkerschmid@users.sourceforge.net

July 7, 2009

## 1 Introduction

Quantitative analysis of perfusion imaging using dynamic contrast-enhanced MRI (DCE-MRI) is achieved through a series of processing steps, starting with the raw data acquired from the MRI scanner, and involves a combination of physics, mathematics, engineering and statistics. The purpose of the **dcemri** package is to provide a collection of functions that move the experimental data through all steps of the data analysis pipeline using standard data formats that may be visualized and manipulated across a wide variety of software packages. To this end, the **dcemri** package requires incoming data to be in the ANALYZE 7.5 or NIfTI formats. Data conversion (e.g., from DICOM to NIfTI) must be performed by the user before **dcemri** may be used to summarize the data.

## 2 Data Input

### 2.1 Labelled LR Standard (MNI152) Images in NIfTI Format

The first example of reading in, and displaying, medical imaging data in NIfTI format (`avg152T1_LR_nifti.nii.gz`) was obtained from the NIfTI website (nifti.nimh.nih.gov/nifti-1/). Successful execution of the command

```
> mni <- read.img("avg152T1_LR_nifti.nii.gz")
> dim(mni)

[1]  91 109  91
```

produces a 3D array of the image data that may be displayed in a 10×10 grid of images (Figure 1).

The second example of reading in, and displaying, medical imaging data in NIfTI format (`avg152T1_RL_nifti.nii`) was also obtained from the NIfTI website (nifti.nimh.nih.gov/nifti-1/). Successful execution of the command

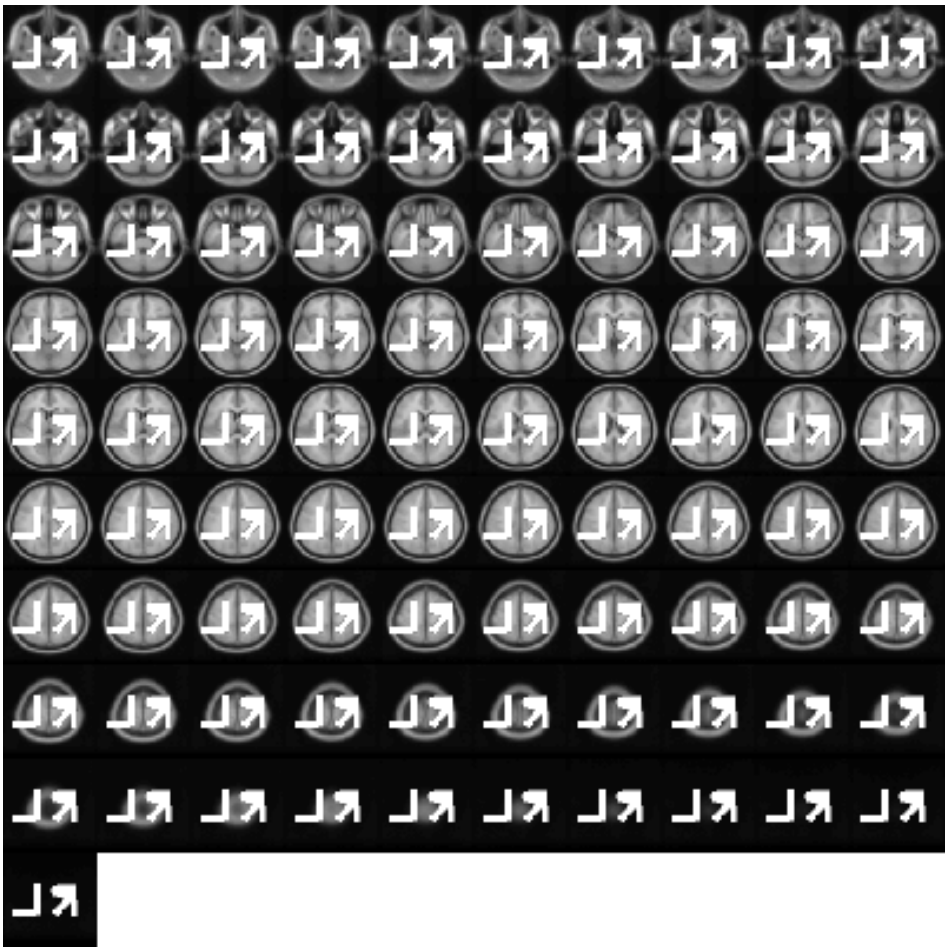

Figure 1: Axial slices of MNI volume `avg152T1_LR_nifti` stored in radiological convention.

```
> mni <- read.img("avg152T1_RL_nifti.nii.gz")
> dim(mni)

[1]  91 109  91
```

produces a 3D array of the image data that may be displayed in a 10×10 grid of images (Figure 2).

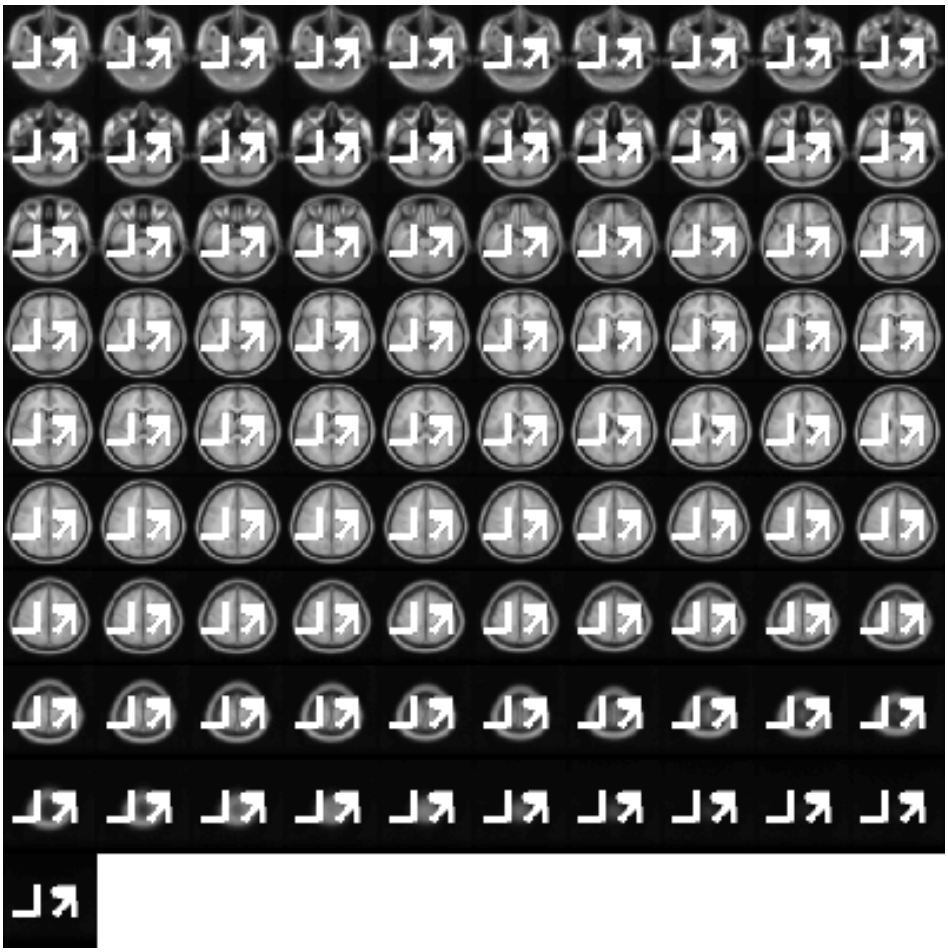

Figure 2: Axial slices of MNI volume `avg152T1_RL_nifti` stored in neurological convention.

The first image (LR) is stored in radiological convention. The second image (RL) is stored in neurological convention. Any NIfTI-1 compliant viewing software should display these images identically.

## 2.2 Simple Time-series or Multi-volume Image

This is an example of reading in, and displaying, a four-dimensional medical imaging data set in NIfTI format (`filtered_func_data.nii`) obtained from the NIfTI website (nifti.nimh.nih.gov/nifti-1/). Successful execution of the command

```
> ffd <- read.img("filtered_func_data.nii.gz")
> dim(ffd)

[1]  64  64  21 180
```

produces a four-dimensional (4D) array of imaging data that may be displayed in a 5×5 grid of images (Figure 3). The first three dimensions are spatial locations of the voxel (volume element) and the fourth dimension is time.

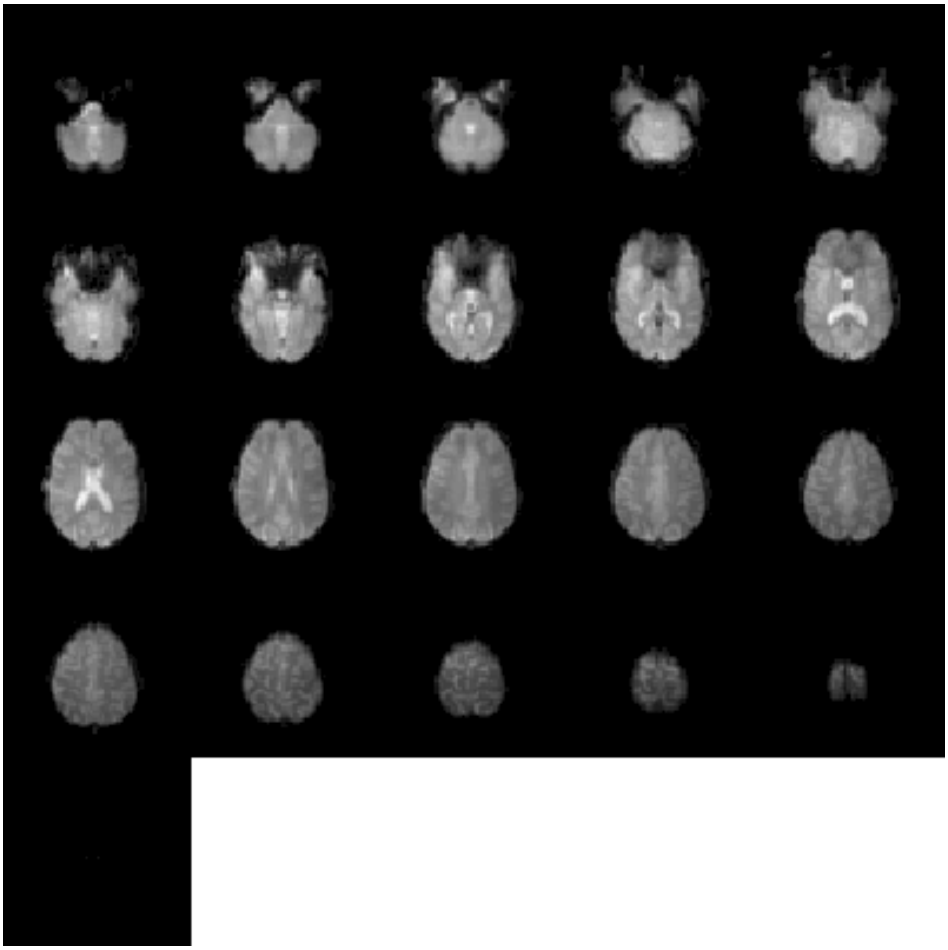

Figure 3: Axial slices of the functional MRI "volume" `filtered_func_data` from the first acquisition.

### 2.3 Statistic Image

This is an example of reading in and displaying a statistical image so that it may be overlayed on the EPI (echo planar imaging) data taken from the functional MRI experiment. The original NIfTI files (`filtereted_func_data.nii` and `zstat1.nii`) were obtained from the NIfTI website (nifti.nimh.nih.gov/nifti-1/). Successful execution of the command

```
> zstat1 <- read.img("zstat1.nii.gz")
> dim(zstat1)

[1] 64 64 21
```

produces a 3D array of parameter estimates (essentially coefficients from a linear regression performed at each voxel) that may be overlayed on the original data for anatomical reference (Figure 4).

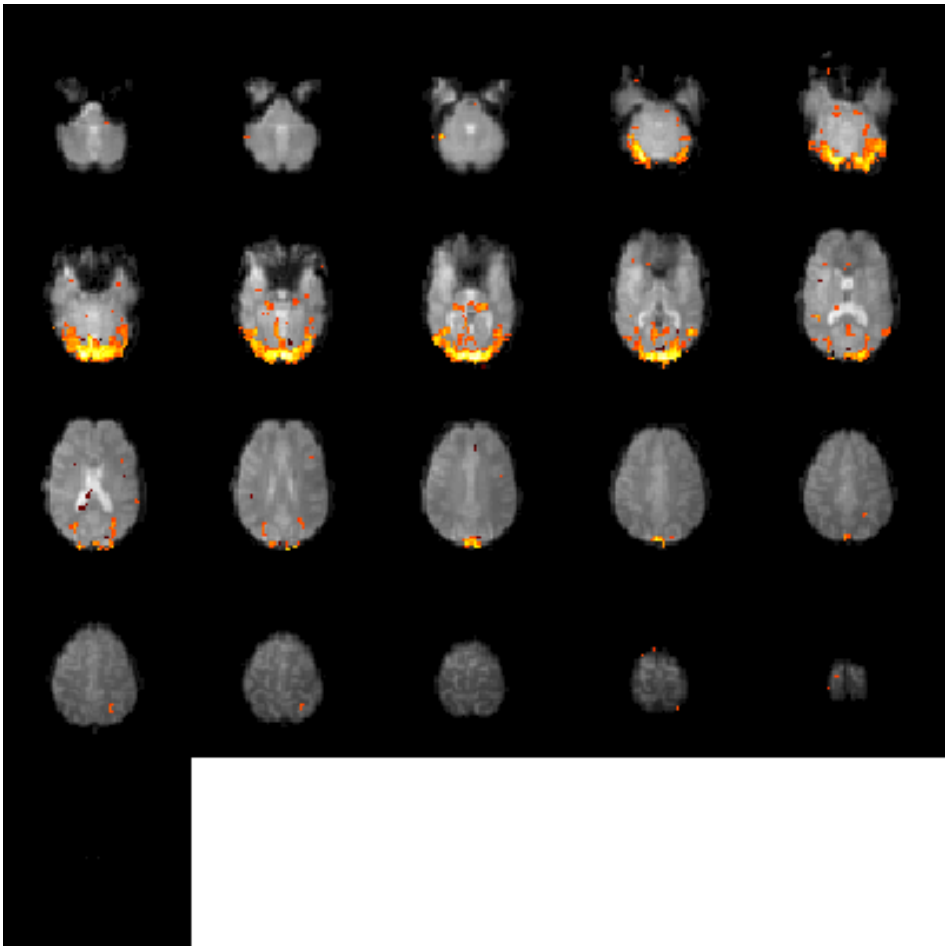

Figure 4: Axial slices of the functional MRI data with with the statistical image overlayed. The test statistics were thresholded at $|Z| \geq 4$.

## 3 Motion Correction and Co-registration

Basic motion correction within an acquisition, and co-registration between acquired series, is available using template matching (en.wikipedia.org/wiki/Template_matching). A reference volume must be pre-specified where a mask has been applied to remove all voxels that should not be included in the algorithm. Note, only three-dimensional translations are allowed and no interpolation is used (i.e., only whole-voxel translations) at this time.

# 4 T1 Relaxation and Gadolinium Concentration

Estimation of the tissue T1 relaxation rate is the first step in converting signal intensity, obtained in the dynamic acquisition of the DCE-MRI protocol, to contrast agent concentration. The subsequent steps provided here focus on pharmacokinetic modeling and assumes one has converted the dynamic acquisition to contrast agent concentration. Please see Collins and Padhani (2004) for a discussion on this point.

There are a miriad of techniques to quantify T1 using MRI. Currently curve-fitting methods for two popular acquisition schemes are available

- Inversion recovery (www.e-mri.org/mri-sequences/inversion-recovery-stir-flair.html)
- Multiple flip angles (Parker and Padhani, 2003)

Once the tissue T1 relaxation rate has been estimated, the dynamic acquisition is then converted to contrast agent concentration. Note, the B1 field is assumed to be constant (and accurate) when using multiple flip angles to estimate T1. At higher fields strengths (e.g., 3T) the B1 field should be estimated in order to correct the prescribed flip angles.

## 4.1 B1 Mapping Via the Saturated Double-Angle Method

For in vivo MRI at high field ($\geq$ 3 T) it is essential to consider the homogeneity of the active B1 field (B1+). The B1+ field is the transverse, circularly polarized component of B1 that is rotating in the same sense as the magnetization. When exciting or manipulating large collections of spins, nonuniformity in B1+ results in nonuniform treatment of spins. This leads to spatially varying image signal and image contrast and to difficulty in image interpretation and image-based quantification (Cunningham *et al.*, 2006).

## 4.2 Arterial Input Function

Whereas quantitative PET studies routinely perform arterial cannulation (en.wikipedia.org/wiki/Cannula) on the subject in order to characterize the arterial input function (AIF), it has been common to use literature-based AIFs in the DCE-MRI literature. Examples include

- Tofts and Kermode (1984)
- Fritz-Hansen *et al.* (1996)

There has been progress in measuring the AIF using the dynamic acquisition and fitting a parametric model to the observations. Recent models include

- Parker *et al.* (2006)
- Orton *et al.* (2008)

**dcemri** has incorporated all parametric models given above for the AIF, except Parker *et al.* (2006), into the kinetic parameter estimation step. While default values for each model are provided, there is also the ability to include user-specified parameters.

## 5 Kinetic Parameter Estimation

The standard Kety model, a single-compartment model, or the extended Kety model, the standard Kety model with an extra "vascular" term, form the collection of basic parametric models one can apply using **dcemri**. Regardless of which parametric model is chosen for the biological system, the contrast agent concentration curve at each voxel in the region of interest (ROI) is approximated using the convolution of an arterial input function (AIF) and the standard/extended Kety model.

Parameter estimation is achieved using one of two options in the current version of this software:

- Non-linear regression (en.wikipedia.org/wiki/Non-linear_regression) using non-linear least squares (en.wikipedia.org/wiki/Non-linear_least_squares)
- Bayesian estimation (en.wikipedia.org/wiki/Bayes_theorem) using Markov chain Monte Carlo (MCMC) (en.wikipedia.org/wiki/Markov_chain_Monte_Carlo)

Least-square estimates of the kinetic parameters $K^{\text{trans}}$ and $k_{\text{ep}}$ (also $v_{\text{p}}$ for the extended Kety model) are provided in `dce.nlreg` while the posterior median is provided in `dce.bayes`. When using Bayesian estimation all samples from the joint posterior distribution are also provided, allowing one to interrogate the empirical probability density function (PDF) of the parameter estimates.

## 6 Statistical Inference

No specific support is provided for hypothesis testing in **dcemri**. We recommend one uses builtin facilities in R to perform ANOVA (analysis of variance) or mixed-effects models based on statistical summaries of the kinetic parameters over the ROI per subject per visit. An alternative to this traditional approach is to analyze an entire study using a Bayesian hierarchical model (en.wikipedia.org/wiki/Hierarchical_Bayes_model) in **PILFER** (pilfer.sourceforge.net).

One may also question the rationale for hypothesis testing in only one kinetic parameter. Preliminary work has been performed in looking at the joint response to treatment of both $K^{\text{trans}}$ and $k_{\text{ep}}$ in DCE-MRI by O'Connor *et al.* (2010).

## References

Collins, D. J. and A. R. Padhani (2004). Dynamic magnetic resonance imaging of tumor perfusion. *IEEE Engineering in Biology and Medicine Magazine*, 65–83.

Cunningham, C., J. Pauly, and K. Nayak (2006). Saturated double-angle method for rapid B1+ mapping. *Magnetic Resonance in Medicine 55*, 1326–1333.

Fritz-Hansen, T., E. Rostrup, H. B. W. Larsson, L. Søndergaard, P. Ring, and O. Henriksen (1996). Measurement of the arterial concentration of Gd-DTPA using MRI: A step toward quantitative perfusion imaging. *Magnetic Resonance in Medicine 36*, 225–231.

O'Connor, E., N. Fieller, A. Holmes, J. C. Waterton, and E. Ainscow (2010). Functional principal component analyses of biomedical images as outcome measures. *Journal of the Royal Statistical Society C (Applied Statistics). in press.*

Orton, M. R., J. A. d'Arcy, S. Walker-Samuel, D. J. Hawkes, D. Atkinson, D. J. Collins, and M. O. Leach (2008). Computationally efficient vascular input function models for quantitative kinetic modelling using DCE-MRI. *Physics in Medicine and Biology 53*, 1225–1239.

Parker, G. J. M. and A. R. Padhani (2003). $T_1$-w DCE-MRI: $T_1$-weighted dynamic contrast-enhanced MRI. In P. Tofts (Ed.), *Quantitative MRI of the Brain: Measuring Changes Caused by Disease*, Chapter 10, pp. 341–364. Chichester, UK: Wiley.

Parker, G. J. M., C. Roberts, A. Macdonald, G. A. Buonaccorsi, S. Cheung, D. L. Buckley, A. Jackson, Y. Watson, K. Davies, and G. C. Jayson (2006). Experimentally-derived functional form for a population-averaged high-temporal-resolution arterial input function for dynamic contrast-enhanced MRI. *Magnetic Resonance in Medicine 56*, 993–1000.

Tofts, P. S. and A. G. Kermode (1984). Measurement of the blood-brain barrier permeability and leakage space using dynamic MR imaging. 1. Fundamental concepts. *Magnetic Resonance in Medicine 17*(2), 357–367.